

# MIRACLE AND CHAMP: SOME RESULTS; MIRACLE AND SWARM: SOME OPPORTUNITIES

O. Amm, L. Juusola, A. Viljanen, and K. Kauristie

*Finnish Meteorological Institute, Space Physics Program, P.O. Box 503, FIN-00101 Helsinki, Finland  
tel: +358 9 1929-4689/fax: +358 9 1929-4603, Email: Olaf.Amm@fmi.fi*

## ABSTRACT

During the CHAMP satellite mission, a new technique has been developed for deriving zonal and meridional ionospheric currents, as well as field-aligned currents from the satellite magnetic data, on comparable spatial scales. This technique is based on 1-dimensional spherical elementary current systems (1D SECS), and uses the assumption that all horizontal gradients vanish in a certain direction. As examples of the results of this technique, we present semiglobal statistical distributions of the currents, as well as of the ionospheric Hall-to-Pedersen conductance ratio. With the SWARM mission, data from two or three closeby satellites are available, so that gradients of the fields can be inferred. Moreover, also electric field measurements are available. We show how with such data the previously derived techniques can be extended to treat non-1D situations as well. We further emphasize the cooperation possibilities between SWARM and ground-based instruments.

## 1. INTRODUCTION

Two-dimensional spherical elementary current systems (2D SECS) have first been introduced by [1]. They consist of a curl-free (cf) and a divergence-free (df) elementary system as illustrated in Fig. 1. By superposition of such elementary systems, with the positions of their poles distributed over the area of interest, and each elementary system having a different scaling factor  $I_{0,cf}$  or  $I_{0,df}$  (cf. Fig. 1), any continuously differentiable current (or generally vector) field on a sphere can be reproduced. The elementary systems are thus complete basis functions for such vector fields. If a vector field is *a priori* known to be either curl-free or divergence-free (like the horizontal equivalent currents below the ionosphere, which are caused by the actual ionospheric current system), only one type of elementary systems needs to be used, and thus 50% of the free parameters of the expansion are removed.

2D SECS have been widely used for different purposes in Space Physics, e.g., for the upward continuation of external magnetic field disturbances from the ground to the ionosphere [2], or for the separation of internal and external components of the ground magnetic field disturbance [3].

In the case that data are only available along a single line, e.g., for a meridional ground magnetometer chain, or for single satellite data, 2D modeling is not available. In that case, using the 1D assumption that all horizontal gradients vanish in a certain direction, the ionospheric currents can be modeled using 1D SECS (Fig. 2). Note that the mentioned direction does not necessarily need to be

perpendicular to the direction in which data are available (e.g., the satellite track, or the direction of a ground magnetometer chain), and that it is possible from the magnetic data itself to estimate an optimum 1D direction, as well as how suitable the 1D assumption is for a particular case. 1D SECS have first been introduced by [4]. They are derived by integrating all 2D SECS at a chosen, fixed latitude  $\vartheta_0$ , over the full longitude circle of the sphere. That fixed latitude is then called the "pole" latitude of the 1D SECS. Like 2D SECS are complete basis functions for general vector fields on a sphere, 1D SECS are complete basis functions for all vector fields on a sphere that satisfy the chosen 1D assumption.

Both for 1D and 2D SECS, the magnetic field effect of the elementary systems at any position below or above the ionosphere can be calculated using analytical expressions. Therefore, it is possible to deduce the ionospheric current systems and field-aligned currents (FAC) by optimally matching the measured disturbance magnetic fields using superpositions of the SECS. This inversion procedure can be applied with magnetic data from above the ionosphere (satellites) or below the ionosphere (ground magnetometers) separately, but also with a combination of both, if available.

In addition to naturally dividing up curl-free and divergence-free parts of a vector field, among the advantages of SECS are that they constitute local basis functions (so that it is not necessary to model basis functions far away from the actual region of interest), and that the density and location of the SECS poles can be freely chosen (and thus be adjusted to the density of the available data points, or to the structure of the data themselves). Particular in comparison to spherical (cap) harmonic techniques, for SECS it is not necessary to globally select a smallest and largest wavelength that can be modeled.

## 2. SOME CHAMP RESULTS USING THE 1D SECS TECHNIQUE

The 1D SECS technique has been applied to over 6000 passes of the CHAMP satellite between  $55^\circ$  and  $76.5^\circ$  northern magnetic latitude during the years 2001 and 2002. The overpasses were selected such that the 1D criterium was sufficiently matched. The results were used to construct statistics of the full ionospheric and field-aligned current system over the northern auroral zone, and binned with respect to different geomagnetic activity levels, season, and interplanetary magnetic field (IMF) conditions. Further, under the required 1D assumption, statistical relations between the magnitude of the zonal ionospheric currents and the Hall-to-Pedersen conductance ratio have been established. These statistical

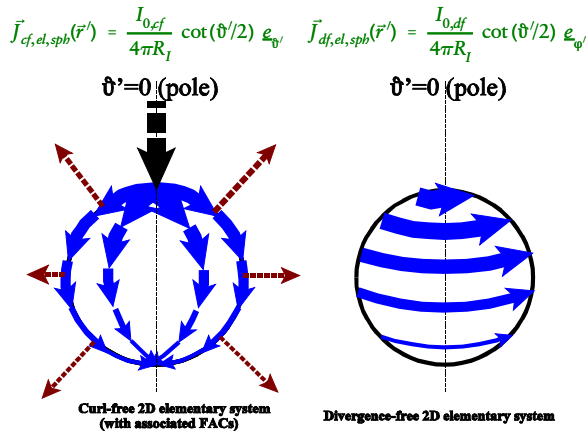
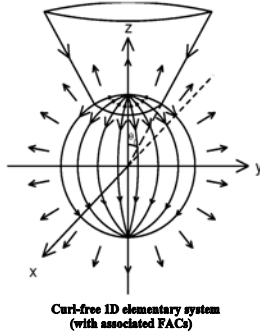
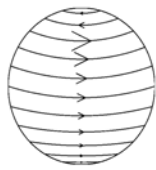


Figure 1. Sketch of curl-free (left) and divergence-free (right) 2D spherical elementary current systems (SECS), with defining equations on the top, given in the spherical coordinate system of the pole of each elementary system.

$$\vec{J}_{cf,el,sph}(\vartheta, \vartheta_0) = \frac{I_{0,cf}}{2R_1} \hat{e}_{\vartheta} \begin{cases} -\tan(\vartheta/2), \vartheta < \vartheta_0 \\ \cot(\vartheta/2), \vartheta > \vartheta_0 \end{cases}$$



$$\vec{J}_{df,el,sph}(\vartheta, \vartheta_0) = \frac{I_{0,df}}{2R_1} \hat{e}_{\varphi} \begin{cases} -\tan(\vartheta/2), \vartheta < \vartheta_0 \\ \cot(\vartheta/2), \vartheta > \vartheta_0 \end{cases}$$



Divergence-free 1D elementary system

Figure 2. Sketch of curl-free (left) and divergence-free (right) 1D spherical elementary current systems (SECS), with defining equations on the top, given in the global spherical coordinate system (e.g., geographic). The latitude  $\vartheta_0$  is called the “pole latitude” of the 1D SECS.

relations have been refined for different geomagnetic activity levels, seasons, and for the eastward and westward electrojet domains. Full details of this study can be found in [5]. Here we only present a few result plots in order to demonstrate the power of the SECS technique.

Fig. 3 shows the average statistical distribution of  $j_r$  (FAC, positive upwards), and of  $J_{\vartheta}$  and  $J_{\varphi}$  (ionospheric

sheet current density, positive southwards and eastwards, respectively), for all 6112 overpasses of our data set that match the imposed 1D condition. This can be regarded as a test for the output of our technique. Clearly, the most prominent and well-known average features of the polar current system are visible in our results: The region 1 and region 2 FAC areas are seen with opposite polarity in the morning and evening sector, as well as the connection of the region 2 morning side and region 1 evening side upward FAC along the Harang discontinuity around midnight. The westward and eastward electrojet domains in the morning and afternoon sector, respectively, are also very well reproduced.

Two differences of our results as compared to previous studies are worth noticing: First, we also derive  $J_{\vartheta}$  directly from the magnetic data. Second, although  $j_r$  and  $J_{\vartheta}$  are derived from the curl-free current system that includes the FAC flowing close to the satellite, and  $J_{\varphi}$  is derived from the divergence-free current system that only flows in the ionosphere, i.e.,  $\sim 300$ - $350$  km below the satellite, all parts of the current system in Fig. 3 are derived on a matching spatial scale. This makes it possible to combine them, as it is required for the calculation of the Hall-to-Pedersen conductance ratio  $\alpha$ , for which the ratio  $J_{\varphi}/J_{\vartheta}$  is needed (for more details see [5]).

Fig. 4 shows the results of the statistical study of the relation between  $J_{\varphi}$  and  $\alpha$ , under northern winter, equinox and summer conditions. The red and blue curves show the best fit relations for the eastward and westward electrojet domain, respectively, while the bars represent the standard deviation for each value of  $J_{\varphi}$ . With increasing zonal currents,  $\alpha$  quickly increases to values between 1.5 and 2. When  $J_{\varphi}$  is increased further, the increase of  $\alpha$  slows down and in some cases almost reaches a saturation level. It is noticeable that  $\alpha$  tends to reach higher values in the westward electrojet than in the eastward one, particularly under winter and equinox conditions.

Finally, using the overpasses of CHAMP over the MIRACLE network of ground-based instruments [6], which includes the IMAGE magnetometer network, Fig. 5 presents a comparison of  $J_{\varphi}$  as derived from the CHAMP data with the 1D SECS technique, and the zonal component of the ionospheric equivalent currents,  $J_{\varphi,eq}$ , as derived from the ground magnetometers with the 2D SECS upward continuation technique [2]. It can be seen that the current densities derived from ground and space match each other very well, with a correlation coefficient of 0.9. The small residual deviation is most likely caused by the fact that many of the events that match the definition of our 1D criterium for the CHAMP data analysis are not “perfectly” 1D. In that case, naturally the 1D and 2D data analyses give slightly different outputs. Still, the fit between the two data sets is so close that for most applications they can be regarded as practically equal. This means that the statistics for  $\alpha$  as presented in Fig. 4 can also be applied with  $J_{\varphi,eq}$  values derived from ground magnetometers, at least when the geometry of the ionospheric currents is close to 1D.

### 3. SOME NEW OPPORTUNITIES WITH SWARM

As compared to a single satellite mission like CHAMP,

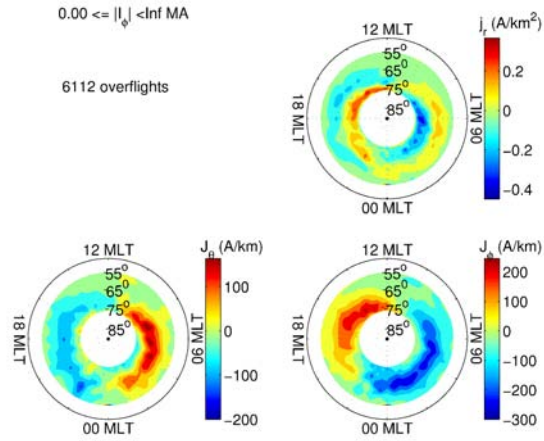


Figure 3. Average statistical distribution of  $j_r$  (FAC, positive upwards),  $J_\phi$  and  $J_\phi$  (ionospheric sheet current density, positive southwards and eastwards, respectively), for all 6112 overpasses of our data set that match the imposed 1D condition.

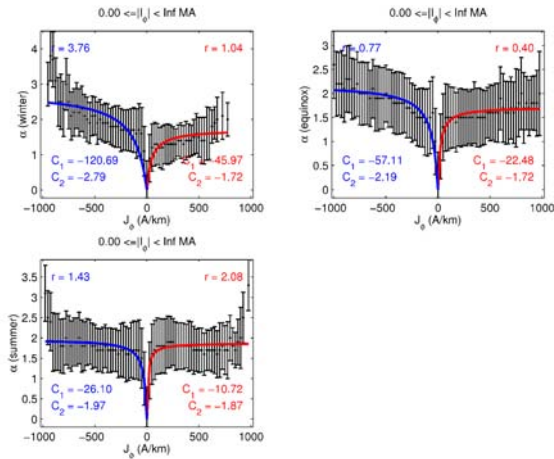


Figure 4. Statistical relation between  $J_\phi$  and  $\alpha$ , for winter (upper left), equinox (upper right), and summer (lower left) conditions. The black points in the center are median values, the bars represent the standard deviation. The red and blue curves are fits for the eastward and westward electrojet domains, respectively.

the upcoming SWARM mission offers the following exciting main new features: First, two satellites, and during special constellations three, are located closeby in the ionosphere, thus allowing to measure gradients of ionospheric electrodynamic parameters *in situ*. Second, the SWARM satellites will fly an instrument to observe the electric field in the F-region of the ionosphere. The first new feature allows us to extend the class of events for which we can deduce the ionospheric currents and FAC from the satellite data from close-to-1D events towards 2D events. The second new feature allows to compare the ionospheric electric field at SWARM altitudes, i.e., at 450-550 km altitude, with measurements of the electric field at lower altitudes in the E-region, as observed by coherent scatter radars, and thereby obtain new detailed knowledge of ionospheric physics. Further it

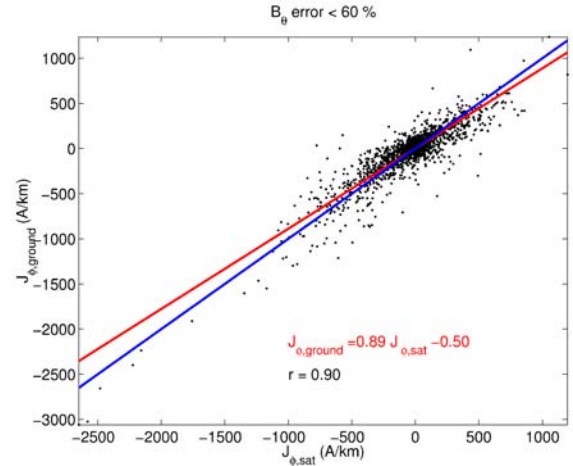


Figure 5. Comparison of zonal currents derived from the CHAMP satellite data with the 1D SECS technique ( $J_{\phi,sat}$ ) with zonal ionospheric equivalent currents derived from the MIRACLE ground-based data using the 2D SECS upward continuation technique ( $J_{\phi,ground}$ ). The blue curve would result if both quantities were exactly equal, and the red curve indicates the best fit.

allows to calculate ionospheric conductances. These two new possibilities will be sketched in the following.

If approximately as many satellites were available closeby in the ionosphere as there are ground magnetometers in a network like MIRACLE [6], it would be natural and feasible to use the full 2D SECS technique, as developed in [1]-[3] for ground magnetometer data, also with the satellite data. With only 2 (or at times 3) satellites, however, this approach would lead to the problem that the amount of data may be insufficient to define any arbitrary 2D current system in the vicinity of the satellite path. Further, due to the limitations of the zonal coverage of the satellite data for any single event (usually 2 about parallel satellite paths with a 160 km separation), using solely 2D SECS in such a zonally narrow area may lead to problems in modeling actual 1D situations (which are, as our CHAMP studies have shown, quite frequent).

Therefore, in order to model ionospheric currents and FAC with SWARM data, we propose a hybrid technique such that a chain of 1D SECS is used like for single satellite data, and in addition some 2D SECS poles are allowed on top of and in the vicinity of that 1D chain, as illustrated in Fig. 6. The chain of 1D SECS will assure that the often close-to-1D background electrojet can be well modeled, while the 2D SECS poles allow to model any 2D variations on top of that background electrojet in the vicinity of the satellite path. It should be noted that with this combination of 1D and 2D SECS, the total system of basis functions is to some extent linearly dependent. While it is not expected that this leads to serious problems in practice, the proposed technique needs to be carefully checked with synthetic data sets before use with actual SWARM data. This work will be carried out in the near future.

Once the true ionospheric currents are deduced from the SWARM data, together with the measurements of the

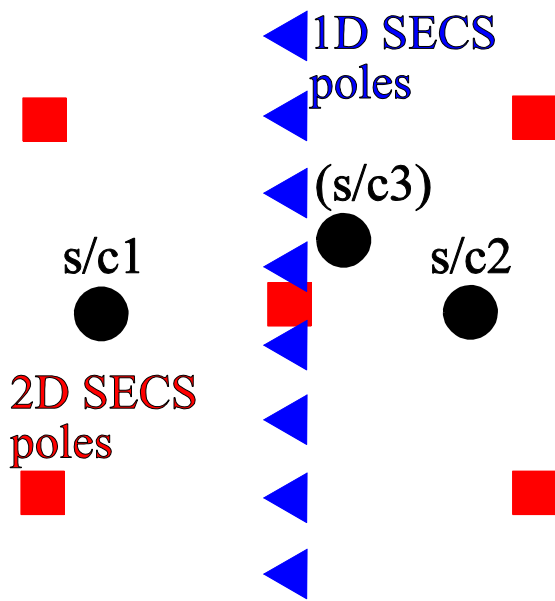


Figure 6. Illustration of hybrid 1D/2D SECS technique for modeling of SWARM data: A chain of 1D SECS (blue triangles) is used to model the background electrojet, and in addition to that some 2D SECS (red squares) are allowed in order to model 2D variations of the currents in the vicinity of the spacecraft tracks. The black circles illustrate the spacecraft positions.

electric field, the ionospheric conductances can directly be calculated by the ionospheric Ohm's law.

While with respect to the large-scale electric field in the ionosphere, in first order it is a good approximation to consider the Earth's magnetic field lines as equipotentials, which means that the electric field in the ionosphere does not change with altitude along them, on mesoscales and smaller scales a number of processes may act to make the electric field altitude dependent, particularly in the lower ionosphere. Such processes include inductive electric fields, the effect of space charges and a significant field-aligned resistance in the lower ionosphere, and the scale dependence of the current closure and electric fields as a function of altitude [e.g., 7, 8].

By comparison of data of the ionospheric electric field at lower altitudes in the E-region, as they can be made, e.g., with the STARE or SuperDARN coherent scatter radars [9, 10], with SWARM data, much can be learnt about the detailed processes that influence the ionospheric electric field on mesoscales. This is particularly the case because, in contrast to earlier satellite missions, SWARM is able also to measure gradients of the ionospheric electric field in the F-layer.

#### 4. CALIBRATION OF SWARM DATA WITH GROUND-BASED RADAR AND MAGNETOMETER DATA

Finally we mention about a possibility to calibrate the ionospheric and field-aligned currents as deduced from

the SWARM data, with data of the MIRACLE ground-based network: By using combined 2D observations of the ground magnetic field disturbance and the ionospheric electric field, and an estimate of  $\alpha$ , the 2D distributions of true currents and FAC can be calculated using the method of characteristics [e.g., 11]. These results can be compared with the results of the approach described above to deduce the 2D true current distribution from the SWARM data, in order to test its accuracy, and to check how well and possibly until which limit the SWARM approach is able to capture the full 2D distribution of the ionospheric parameters.

The MIRACLE network is particularly suited for such an approach because it provides dense 2D ground-based observations of the ionospheric electric field and of the ground magnetic disturbance. However, the sketched approach assumes that a replacement for the STARE radar (which was discontinued in 2005) will be implemented to MIRACLE before the launch of the SWARM mission.

#### 5. SUMMARY AND CONCLUSIONS

In this paper, we have demonstrated that using the 1D SECS technique with a single satellite mission like CHAMP, we are able to derive the ionospheric currents and FAC with very good accuracy for situations that satisfy a 1D condition. All parts of the current system are directly inferred from the satellite magnetic data, on a comparable spatial scale. Further, under the same condition we are able to calculate the Hall-to-Pedersen conductance ratio  $\alpha$ . For all the inferred parameters, statistical distributions have been composed for the northern auroral zone, and binned according to several relevant parameters of the Geospace environment.

For the SWARM mission we will be able to extend the realm of the situations that are possible to model from 1D situations towards 2D ones. As most of the time, only 2 satellites are available closeby, we propose to use a hybrid 1D/2D SECS technique in order to model the current systems. This approach needs to be tested with synthetic data before use with real data. Together with ionospheric electric field data, also the ionospheric conductances can then be calculated directly from Ohm's law.

Finally, the availability of simultaneous ground magnetic and ionospheric electric field data from the MIRACLE network would give us the possibility to infer the 2D current system and FAC independently, using the ground-based data for situations when SWARM passes over the MIRACLE network. This would allow to calibrate the new technique for the SWARM magnetic field data analysis, and to test how well it can handle 2D situations.

#### 6. REFERENCES

1. Amm, O., Ionospheric elementary current systems in spherical coordinates and their application, *J. Geomag. Geoelectr.*, 49, 947, 1997.
2. Amm, O., and Viljanen, A., Ionospheric disturbance magnetic field continuation from the ground to the

- ionosphere using spherical elementary current systems, *Earth Planets Space*, 51, 431, 1999.
3. Pulkkinen, A., Amm, O., Viljanen, A., and BEAR Working Group, Separation of the geomagnetic variation field on the ground into external and internal parts using the spherical elementary current system method, *Earth Planets Space*, 55, 117, 2003.
  4. Vanhamäki, H., Amm, O., and Viljanen, A., 1-dimensional upward continuation of the ground magnetic field disturbance using spherical elementary current systems, *Earth Planets Space*, 55, 613, 2003.
  5. Juusola, L., Amm, O., Kauristie, K., and Viljanen, A., Estimating the Hall to Pedersen conductance ratio from ground and satellite magnetic data, *Ann. Geophys.*, 2006 (submitted).
  6. Syrjäsoo, M., Pulkkinen, T. I., Pellinen, R. J., Janhunen, P., Kauristie, K., Viljanen, A., Opgenoorth, H.J., Karlsson, P., Wallman, S., Eglitis, P., Amm, O., Nielsen, E., and Thomas, C., Observations of substorm electrodynamics using the MIRACLE network, *Proc. Fourth International Conference on Substorms (ICS-4)*, Lake Hamana, Japan, March 9 - 13, 1998.
  7. Brekke, A., *Physics of the upper polar atmosphere*, Wiley-Praxis series in Atmospheric Physics, Chichester, United Kingdom, 1997.
  8. Vanhamäki, H., Viljanen, A., and Amm, O., Induction effects on ionospheric electric and magnetic fields, *Ann. Geophys.*, 23, 1735, 2005.
  9. Greenwald, R.A., Weiss, W., Nielsen, E., and Thomson, N.R.: STARE: A new radar backscatter experiment in northern Scandinavia, *Radio Sci.*, 13, 1021, 1978.
  10. Greenwald, R. A., Baker, K.B., Dudeney, J.R., Pinnock, M., Jones, T.B., Thomas, E.C., Villain, J.-P., Cerisier, J.-C., Senior, C., Hanuise, C., Hunsucker, R.D., Sofko, G., Koehler, J., Nielsen, E., Pellinen, R., Walker, A.D.M, Sato, N., and Yamagishi, H., DARN/ SuperDARN: A global view of the dynamics of high-latitude convection, *Space Sci. Rev.*, 71, 761, 1995.
  11. Amm, O., Method of characteristics in spherical geometry applied to a Harang discontinuity situation, *Ann. Geophys.*, 16, 413, 1998.